Journal of Naval Architecture and Marine Engineering
December, 2006
http://jname.8m.net

NUMERICAL SIMULATION OF ADVANCED ADSORPTION REFRIGERATION CHILLER WITH MASS RECOVERY

M.Z.I. Khan[1], S. Sultana[2], A. Akisawa[1], T. Kashiwagi[1]

[1]Graduate School of Bio-Applications and Systems Engineering, Tokyo University of A. & T., 2-24-16, Naka-machi, Koganei-shi, Tokyo 184-8588, Japan
[2]Department of Mathematics, Stamford University, Dhaka, Bangladesh

Abstract

This paper investigates the thermodynamic framework of a three-bed advanced adsorption chiller, where the mass recovery scheme has been utilized such that the performances of this chiller could be improved and a CFC-free-based sorption chiller driven by the low-grade waste heat or any renewable energy source can be developed for the next generation of refrigeration. Silica gel-water is chosen as adsorbent-refrigerant pair. The three-bed adsorption chiller comprises with three sorption elements (SEs), one evaporator and one condenser. The configuration of SE1 and SE2 are identical, but the configuration of SE3 is taken as half of SE1 or SE2. Mass recovery process occurs between SE3 with either SE1 or SE2 and no mass recovery between SE1 and SE2 occurs. The mathematical model shown herein is solved numerically. In the present numerical solution, the heat source temperature variation is taken from 50 to 90ºC along with coolant inlet temperature at 30ºC and the chilled water inlet temperature at 14ºC. A cycle simulation computer program is constructed to analyze the influence of operating conditions (hot and cooling water temperature) on COP (coefficient of performance), SCP (specific cooling power), η (chiller efficiency) and chilled water outlet temperature.

Keywords: Adsorption; COP; SCP; Mass recovery; Silica gel-water

NOMENCLATURE

A	area (m^2)	*Subscripts*	
C_p	specific heat ($J\ kg^{-1}\ K^{-1}$)	ads	adsorber, adsorption
D_{so}	pre-exponential constant ($m^2 s^{-1}$)	cond	condenser
E_a	activation energy (Jkg^{-1})	chill	chilled water
L	latent heat of vaporization ($J\ kg^{-1}$)	cw	cooling water
$\dot{m}$	mass flow rate ($kg\ s^{-1}$)	des	desorber, desorption
P_s	saturated vapor pressure (Pa)	eva	evaporator
q	concentration (kg / kg)	hex	heat exchanger
q^*	concentration equilibrium (kg / kg)	hw	hot water
Q_{st}	isosteric heat of adsorption ($J\ kg^{-1}$)	in	inlet
R	gas constant ($Jkg^{-1}K^{-1}$)	out	outlet
R_p	average radius of a particle (m)	s	silica gel
T	temperature (K)	se	sorption element
t	time (s)	w	water
U	heat transfer coefficient ($W\ m^{-2}\ K^{-1}$)	wv	water vapor
W	weight (kg)		

1. Introduction

Since the Montreal Protocol called for a ban on the use of CFCs, there have been increased research efforts over the last twenty years on the development of refrigeration technologies which address the environmental concerns of ozone layer depletion and global warming. The sorption cooling system is environment-friendly compared with traditional CFC systems as it employs safe and non-polluting refrigerants. The most common thermally-driven sorption cooling system is the gas-liquid absorption system (LiBr–H2O, H2O–NH3) which offers numerous advantages in specific applications. However, such a system possesses certain limitations in operating conditions studied by Douss et al. (1989) and Stitou et al. (2000). Thus, adsorption systems have attracted increased research interests as an alternative cooling solution. However, the main limitation in the commercial application of adsorption systems is its rather low coefficient of performance. In order to improve

the performance of such cooling systems, several advanced cycles have been proposed such as the continuous cycle by Cacciola et al. (1995), cascading cycle by Douss et al. (1989) and Stitou et al. (2000), forced convection cycle by Critoph (1998) and thermal wave cycle by Miles (1989). Wang et al. (2002) incorporated heat and mass recovery processes into the continuous cycle to improve its thermal performance. However, the resulting COP is still rather low being below 1.0. Recently, Leong and Liu (2004) modeled a combined heat and mass recovery adsorption cycle employing a compact zeolite adsorbed bed and obtained COP values which are slightly better than those of Wang et al. (2002). Douss and Meunier (1989) proposed a cascading cycle with a higher COP of 1.06. Stitou et al. (2000) analyzed different cascading cycles which coupled solid–gas reactions with the liquid–gas absorption process. The COP can be increased by more than 30% compared with double-effect absorption cycles. In cascading cycles, different condenser and evaporators are employed for different pairs. The system configuration and operation are inherently more complex compared with continuous cycles. The forced convection and thermal wave cycles are both capable of achieving high COP values. However, for actual engineering application, the operating conditions of these systems are difficult to control. Meunier (1986) studied the system performance of cascading cycle in which an active/methanol cycle is used topped by zeolite/water cycle. To improve the COP value, Shelton et al. (1990) proposed thermal wave regenerative adsorption heat pump. To improve the cooling power, Pons and Poyelle (1999) studied the influence of mass recovery process in conventional two beds adsorption cycle. Later, Wang (2001) investigated the performances of vapor (mass) recovery cycle with activated carbon-methanol as adsorbent/adsorbate pair and demonstrated that the mass recovery cycle is effective for the low regenerating temperature.

In this study, silica gel–water has been selected as the adsorbent–adsorbate pair because of the low regeneration temperature of silica gel and the high latent heat of vaporization of water. Additionally, this working pair is non-toxic and environment friendly. In the present study, a novel strategy of mass recovery cycle is proposed to improve the cooling effect. In the new strategy, mass recovery process occurs between SE3 with either SE1 or SE2 and no mass recovery between SE1 and SE2 occurs. The present strategy is completely different from the conventional mass recovery cycle as there is no heating and cooling process during mass recovery process in conventional mass recovery cycle. In the present strategy additional heating and cooling accelerated the desorption/adsorption process; thus the system provides the better cooling output.

2. Working Principle of the Mass Recovery Chiller

The schematic diagram and time allocation of the proposed three-bed mass recovery chiller are shown in Fig. 1 and Table 1, respectively. The three-bed mass recovery chiller comprises with three sorption elements (SEs) (adsorber/desorber heat exchangers), a condenser, an evaporator, and metalic tubes for hot, cooling and chilled water flows as shown in Fig. 1. The design criteria of the three-bed mass recovery chiller are almost similar to that of the three-bed chiller without mass recovery which is proposed and devoloped by Saha et al. (2003) and (2006). However, in the proposed design, it needs extra piping, which connects two beds during mass recovery. The configeration of SE3 in the three-bed chiller with mass recovery is taken as half size of SE1 or SE2 where SE1 and SE2 are taken same. Operational strategy of the proposed chiller is shown in Table 1. In proposed design, mass recovery process occurs between SE3 with either SE1 or SE2 and no mass recovery between SE1 and SE2 occurs. To complete a full cycle for the proposed system, the chiller needs 10 modes, namely A, B, C, D, E, F, G, H, I and J as can be seen from Table 1.

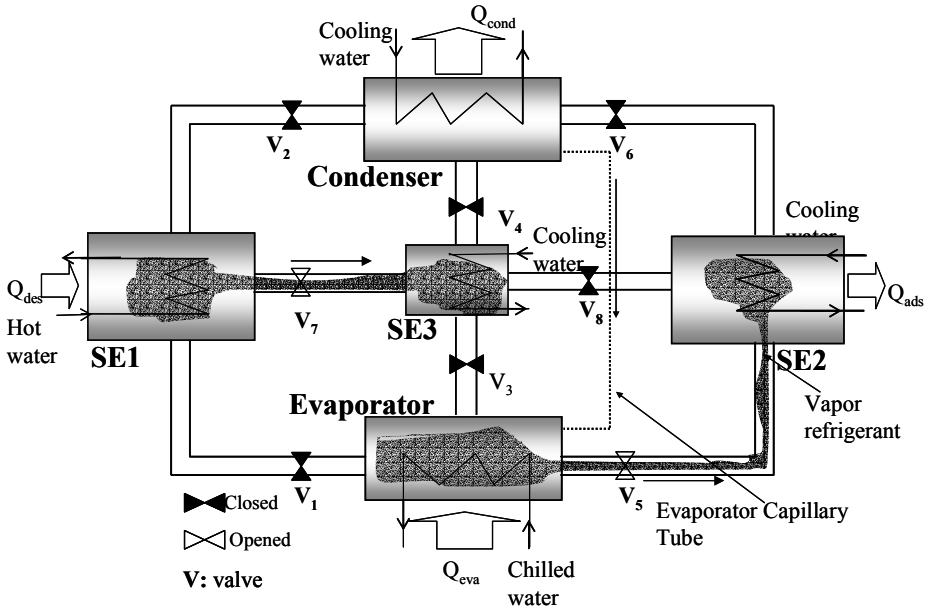

Fig. 1: Schematic of three bed chiller with mass recovery

In mode A, SE1 and SE3 work as desorber. The desorption-condensation process takes place at condenser pressure (P_{cond}). The desorber (SE1, SE3) is heated up to temperature (T_{des}) by heat input Q_{des}, provided by the driving heat source. The resulting refrigerant is cooled down by temperature (T_{cond}) in the condenser by the cooling water, which removes condensation heat, Q_{cond}. SE2 works as adsorber in mode A. In the adsorption-evaporation process, refrigerant (water) in evaporator is evaporated at evaporation temperature, T_{eva}, and seized heat, Q_{eva} from chilled water. The evaporated vapor is adsorbed by adsorbent (silica gel), at which cooling water removes the adsorption heat, Q_{ads}.

Table 1: Operational strategy of three bed chiller with mass recovery

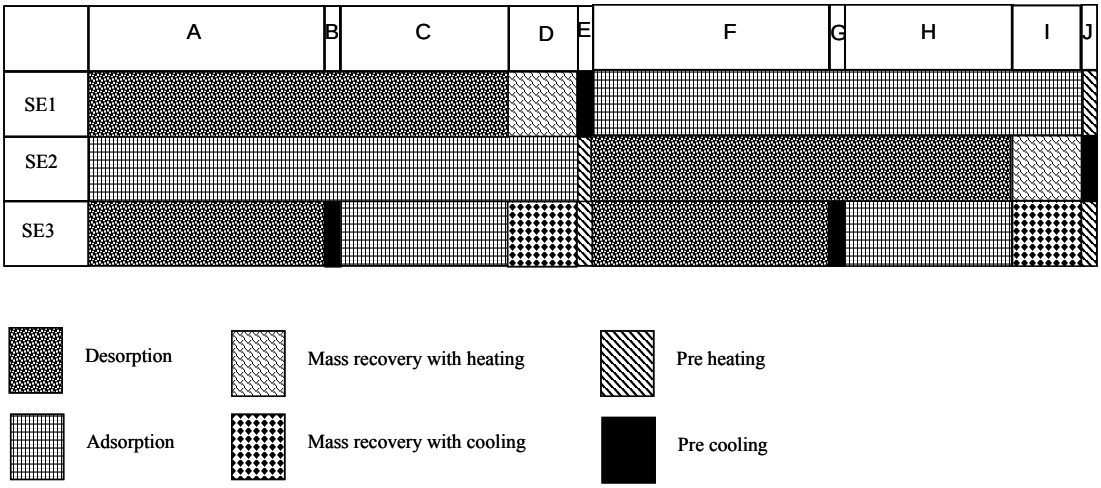

Mode B is the pre-cooling process for SE3. In pre-cooling process, SE3 is isolated from evaporator, condensed or any other beds. Cooling water is supplied to the bed for short time (30s) in this period. SE1 works as desorber and SE2 works as adsorber in mode B also.

Mode C is the adsorption process for SE3, SE2 and desorption process for SE1.

In mode D, SE3 (at the end position of adsorption-evaporation process) and SE1 (at the end position of desorption-condensation process) are connected with each other continuing cooling water and hot water, respectively that can be classified as two-bed mass recovery process. This time SE3 is isolated from evaporator and SE1 is isolated from condensed. Here mass recovery occurs only bed to bed. In this mode SE2 works as adsorber. When the concentration levels of both beds SE3 and SE1 reach in nearly equilibrium levels, then warm up process will start, called mode E (pre-heating or pre-cooling).

In mode E, SE2 and SE3 are heated up by hot water, and SE1 is cooled down by cooling water. When the pressure of SE2 and SE3 are nearly equal to the pressure of condenser then SE2 and SE3 are connected to condenser. When the pressure of SE1 is nearly equal to the pressure of evaporator then SE1 is connected to evaporator.

In mode F, SE2 and SE3 work as desorber and SE1 works as adsorber.

Mode G is the pre-cooling process for SE3. In this mode, SE2 works as desorber and SE1 works as adsorber.

Mode H is the adsorption-evaporation process for SE1 and SE3. SE2 works as desorber in this mode.

In mode I, SE3 (at the end position of adsorption-evaporation process) and SE2 (at the end position of desorption-condensation process) are connected with each other continuing cooling water and hot water, respectively that can be classified as two-bed mass recovery process. When the concentration levels of both beds SE3 and SE2 reach in nearly equilibrium levels, then warm up process will start, called mode J (pre-heating or pre-cooling). SE1 works as adsorber in this mode.

Mode J is the pre-heating/ pre-cooling process for all bed. In this period, SE1 and SE3 are heated up by hot water, SE2 is cooled down by cooling water. Mode J is the last process for all sorption elements (SEs), after this mode, all sorption elements will return to its initial position (Mode A). That's why to complete one cycle, it needs 10 modes.

3. Mathematical Formulation

3.1 Energy balance for the adsorber/desorber heat exchanger

Adsorption and desorption heat balances are described by identical equations, where heat transfer fluid (water) temperature term T_{in} and T_{out} denotes cooling water upon adsorption and hot water upon desorption. T_{hex} denotes reactor bed temperature. The adsorbent bed temperature, pressure and concentration are assumed to be uniform throughout the adsorbent bed. The heat transfer and energy balance equations for the adsorbent bed can be described as follows:

$$T_{w,out} = T_{hex} + (T_{w,in} - T_{hex}) \exp\left(- \frac{U_{hex} A_{hex}}{\dot{m}_w c_{pw}} \right) \tag{1}$$

$$\begin{aligned} &\frac{d}{dt}\left\{\left(W_s (C_{ps} + C_{pw}\, q) + (W_{khex}\, C_{pcu} + W_{fhex}\, C_{pAl})T_{hex}\right\} = W_s Q_{st} \frac{dq}{dt} \\ &- \delta W_s C_{pw} \left\{\gamma(T_{hex} - T_{eva}) + (1-\gamma)(T_{hex} - T_{wv})\right\}\frac{dq}{dt} + \dot{m}_w C_{pw} (T_{w,in} - T_{w,out}) \end{aligned} \tag{2},$$

where, δ is either 0 or 1 depending whether the adsorbent bed is working as desorber or adsorber and γ is either 1 or 0 depending on whether the bed is connected with evaporator or another bed. Equation (1) expresses the importance of heat transfer parameters, namely heat transfer area A_{hex} and heat transfer coefficient U_{hex}. The left hand side of the adsorber/desorber energy balance equations (Eq. 2) provides the amount of sensible heat required to cool or heat the silica-gel (*s*), the water (*w*) contents in bed as well as metallic (*hex*) parts of the heat exchanger during adsorption or desorption. This term accounts for the input/output of sensible heat required by the batched-cycle operation. The first term on the right hand side of Eq. (2) represents the release of adsorption heat or the input of desorption heat, while the second and third terms represent for the sensible heat of the adsorbed vapor. The last term on the right hand side of Eq. (2) indicates the total amount of heat released to the cooling water upon adsorption or provided by the hot water for desorption. Equation (2) does not account for external heat losses to the environment as all the beds are well insulated.

3.2 Energy balance for the evaporator

In the present analysis, it is assumed that the tube bank surface is able to hold a certain maximum amount of condensate and the condensate would flow into the evaporator easily. The heat transfer and energy balance equations for evaporator can be expressed as:

$$T_{chill,out} = T_{eva} + (T_{chill,in} - T_{eva}) \exp\left(- \frac{U_{eva} A_{eva}}{\dot{m}_{chill} C_{p,chill}} \right) \tag{3}$$

$$\begin{aligned} \frac{d}{dt}\left\{\left(W_{eva,w} C_{pw} + W_{eva,hex} C_{p,eva}\right) T_{eva}\right\} = &-LW_s \frac{dq_{ads}}{dt} - W_s C_{pw} (T_{cond} - T_{eva}) \frac{dq_{des}}{dt} \\ &+ \dot{m}_{chill} C_{p,chill} (T_{chill,in} - T_{chill,out}) \end{aligned} \tag{4},$$

where the subscripts *chill* and *eva* indicate chilled water and evaporator respectively. The left hand side of Eq. (4) represents the sensible heat required by the liquid refrigerant (*w*) and the metal of heat exchanger tubes in the evaporator. On the right hand side, the first term gives the latent heat of evaporation (*L*) for the amount of refrigerant adsorbed (dq_{ads}/dt), the second term shows the sensible heat required to cool down the incoming condensate from the condensation temperature T_{cond} to evaporation temperature T_{eva} , and the last term represents the total amount of heat given away by the chilled water.

3.3 Energy balance for the condenser

The heat transfer and energy balance equations for condenser can be expressed as:

$$T_{cond,out} = T_{cond} + (T_{cw,in} - T_{cond}) \exp\left(- \frac{U_{cond} A_{cond}}{\dot{m}_{cw} C_{pw}} \right) \tag{5}$$

$$\frac{d}{dt}\left\{\left(W_{cw,w}C_{pw}+W_{cond,hex}C_{p,cond}\right)T_{cond}\right\}=-LW_s\frac{dq_{des}}{dt} \\ -W_sC_{p,w}\left(T_{des}-T_{cond}\right)\frac{dq_{des}}{dt}+\dot{m}_{cw}C_{pw}\left(T_{cw,in}-T_{cw,out}\right) \quad (6),$$

where the subscripts *cw* and *cond* indicate cooling water and condenser, respectively. The left hand side of Eq. (6) represents the sensible heat required by the metallic parts of heat exchanger tubes due to the temperature variations in the condenser. On the right hand side, the first term gives the latent heat of vaporization (L) for the amount of refrigerant desorbed (dq_{des}/dt), the second term shows the amount of sensible heat requirement to cool down the incoming vapor from the desorber at temperature T_{des} to condenser at temperature T_{cond}, and the last term represents the total amount of heat released to the cooling water.

3.4 Mass balance

Mass and heat balances are based on the assumption that both the temperature and the amount of refrigerant adsorbed are uniform in the adsorbent beds. Since the temperatures in an adsorption cycle are unsteady state, the energy balance equations (Eqs. 2, 4, 6) must account for sensible heat input and/or output during cycle period. The mass balance for the refrigerant can be expressed by neglecting the gas phase as:

$$\frac{dW_{eva,w}}{dt}=-W_s\left(\frac{dq_{des-cond}}{dt}+\frac{dq_{eva-ads}}{dt}\right) \quad (7),$$

where, subscripts *des-cond* and *eva-ads* stand for the vapor flow from desorber to condenser and evaporator to adsorber, respectively.

3.5 Adsorption rate

The adsorption rate is expressed as

$$\frac{dq}{dt}=k_sa_p\times(q^*-q) \quad (8),$$

where, the overall mass transfer coefficient (k_sa_p) for adsorption is given by:

$$k_sa_p=(15D_s)/(R_p)^2 \quad (9).$$

The adsorption rate is considered to be controlled by surface diffusion inside a gel particle and surface diffusivity (D_s) is expressed by Sakoda and Suzuki (1984) as a function of temperature by:

$$D_s=D_{so}\times\exp[-(E_a)/(RT)] \quad (10)$$

and q^* is the amount adsorbed in equilibrium with pressure $P_s(T_w)$ and is chosen from a concise analytical expression of experimental data by the following form:

$$q^*=k\left[P_s(T_w)/P_s(T_s)\right]^{1/n} \quad (11),$$

where $P_s(T_w)$ and $P_s(T_s)$ are the saturation vapor pressure at temperatures T_w (water vapor) and T_s (silica gel), respectively; the parameters k and n are taken as constants. Chihara and Suzuki (1983) obtained experimental values for k and n for the silica gel-water pair as the constants $k = 0.346$ *kg*/*kg* and $n = 1.6$, k denotes the limiting amount adsorbed at $P_s(T_w)/P_s(T_s) = 1$. As the Eq. (11) describes the physical phenomenon of adsorption, the water vapor and the adsorbent temperatures are not equivalent. The refrigerant temperature in the vapor phase is defined by the temperatures of the evaporator (during adsorption) or condenser (in desorption); the adsorbent temperature is determined by the heat transfer fluid (hot or cooling water) temperature. Only for refrigerants in the adsorbed phase are the temperatures of refrigerant and adsorbent taken as equivalent.

Brunauer (1945) states that if a plot of log q^* against log ($P_s(T_w)/P_s(T_s)$) gives a straight line, the adsorption data obey the Freundlich equation. The slope of the straight line then gives $1/n$, and intercept gives log k. For a specific case of carbon monoxide adsorption on coconut charcoal, Brunauer (1945) mentions that both k and n decrease with increasing temperature. In fact, the value of $1/n$ would approach the limiting value of unity when the temperature increases enough for the amount adsorbed (q^*) to become very small.

By comparing Freundlich equation plots to experimental data obtained from the literature of Hubard (1954) and from the manufacturer, NACC (1992), the authors obtained good agreement only in a relatively narrow pressure and temperature range for constant values of k and $1/n$. This led them to adapt the Freundlich equation to the manufacturer's experimental data NACC (1992) for a more precise fit in this study, based on the work of Saha et al. (1995):

$$q^* = A(T_s).\left[P_s(T_w)/P_s(T_s)\right]^{B(T_s)} \quad (12),$$

where,

$$A(T_s) = A0 + A1.T_s + A2.T_s^2 + A3.T_s^3$$

$A0$ = -6.5314
A1 = 0.72452E-01
A 2 = -0.23951E-03
A 3 = 0.25493E-06

$$B(T_s) = B0 + B1.T_s + B2.T_s^2 + B3.T_s^3$$

B 0 = -15.587
B 1 = 0.15915
B 2 = -0.50612E-03
B 3 = 0.53290E-06.

The numerical values of $A0 \sim A3$ and $B0 \sim B3$ are determined by the least-square fits of experimental data. The other values adapted in simulation are presented in Tables 2 and 3.

The saturation vapor pressure and temperature are correlated by Antoine's equation, which can be written as:

$$P_s = 133.32 \times \exp\left(18.3 - \frac{3820}{T - 46.1}\right) \quad (13).$$

Table 2 Baseline Parameters

Values Adopted in Simulation					
Symbol	Value	Unit	Symbol	Value	Unit
A_{bed}	1.45	m^2	R	4.62E+2	J / kg. K
A_{eva}	0.665	m^2	R_p	0.35E–3	m
A_{con}	0.998	m^2	U_{ads}	1380	W / m^2. K
C_{ps}	924	J / kg. K	U_{des}	1540	W / m^2. K
C_{pw}	4.18E+3	J / kg. K	U_{eva}	3550	W / m^2. K
$C_{p,chill}$	4.20E+3	J / kg. K	U_{cond}	4070	W / m^2. K
$C_{p,cu}$	386	J / kg. K	W_s	14	kg
$C_{p,Al}$	905	J / kg. K	W_{khex}	12.67	kg
D_{so}	2.54E–4	m^2 / s	W_{fhex}	5.33	kg
E_a	2.33E+3	J / kg	W_{cw}	5	kg
L	2.50E+6	J / kg	$W_{eva,w}$	25	kg
Q_{st}	2.80E+6	J / kg			

Table 3: Standard operating condition

	Hot water	Cooling water	Chilled water	Time
Temperature (°C)	50 ~ 90	30	14	Total cycle time = 900s, Mass recovery time = 160s, Pre heating/cooling time = 30s.
Flow rate (kg/s)	0.4	0.4(ads)+0.34(cond)	0.11	

3.6 Measurement of system performance

The performance of a three-bed adsorption chiller with mass recovery is mainly characterized by specific cooling power (SCP) which is defined as cooling capacity per kg silica gel, coefficient of performance (COP), waste heat recovery efficiency, η and can be measured by the following equations:

$$\text{Specific Cooling Power} = \dot{m}_{chill} C_w \int_0^{t_{cycle}} \left(T_{chill,in} - T_{chill,out}\right) dt \Big/ W_{s,chiller} \cdot t_{cycle},$$

here, $W_{s,chiller}$ stands for the total mass of silica gel in the chiller.

Coefficient of performance (COP) =

$$\dot{m}_{chill} C_w \int_0^{t_{cycle}} \left(T_{chill,in} - T_{chill,out}\right) dt \Big/ \dot{m}_{hot} C_w \int_0^{t_{cycle}} \left(T_{hot,in} - T_{hot,out}\right) dt,$$

and the Waste Heat Recovery Efficiency, η =

$$\dot{m}_{chill} C_w \int_0^{t_{cycle}} (T_{chill,in} - T_{chill,out}) dt \Big/ \dot{m}_w C_w \int_0^{t_{cycle}} (T_{hot,in} - T_{cool,in}) dt .$$

4. Calculation Procedure

In the present analysis, a cycle simulation computer program is developed to predict the performance of the three-bed chiller with mass recovery. The above mentioned set of coupled equations is solved by finite difference approximation with a time step of one second. The results taken in the study are from the cyclic steady state conditions. A real chiller starts its operation from the unbalance conditions; however, it reaches in balance condition after few cycles. Therefore, an iteration technique is employed in the solution procedure to fix the initial conditions for the cyclic steady state. In the beginning of the solution process, the initial conditions are assumed; however, those are adjusted for the cyclic steady conditions by the iteration process.

When two beds are connected with each other, the vapor pressure is unknown, which are essential for the calculation of adsorption/desorption rate inside the adsorbent beds. In this state, vapor pressure is assumed initially and the amounts of vapor adsorbed/desorbed by the beds are calculated. Conceptually, the desorbed vapor from one reactor bed (SE1) should be equal to the amount of adsorbed vapor by the other reactor bed (SE3). If these amounts are not equal then vapor pressure are adjusted for next iteration. Once the satisfactory convergence criterion is achieved, then process goes for the next time step. The output results have almost no dependency on the assumed initial conditions. The convergence factor is taken as 10^{-3} for all parameters.

5. Results and Discussion

In order to clarify the performance of mass recovery cycle, cycle simulation runs are performed. Since our main interest is to utilize the low grade waste heat as the driving source, the investigation was conducted for hot water between 50 and 90°C. The base line parameters and standard operating conditions for the chiller operation are listed in Table 2 and Table 3, respectively. The effect of operating temperature (hot and cooling water) is calculated by the simulation runs.

5.1 Effect of driving heat source temperature on SCP and COP

Figure 2 shows heat source temperature variation on SCP (specific cooling power). It is seen that SCP for three-bed mass recovery chiller increases with the increase of heat source temperature. This is because the amount of refrigerant circulated increases, due to increased refrigerant desorption with higher driving source temperature. Another reason is that, in the proposed cycle, SE1 and SE2 connect with SE3 one by one during mass recovery, which accelerates cooling effect. In Fig. 3, COP is depicted with the variation of driving heat source temperature. It is seen that COP of the proposed cycle is also increased with the increase of heat source temperature as we observed for SCP. It is already stated that the SCP is improved due to the mass recovery process. The mass recovery process generates more desorption heat and that is transferred from the desorber through desorbed vapor. So, in the low heat source temperature (65-80°C), proposed chiller gives better performance.

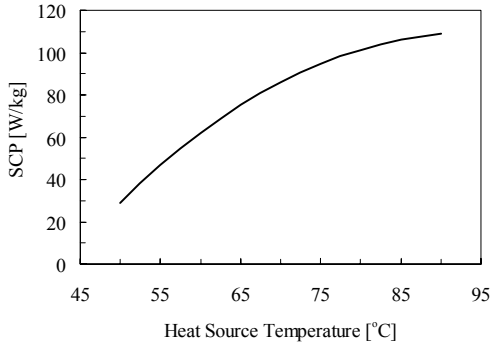

Fig.2 The effect of heat source temperature on specific cooling power.

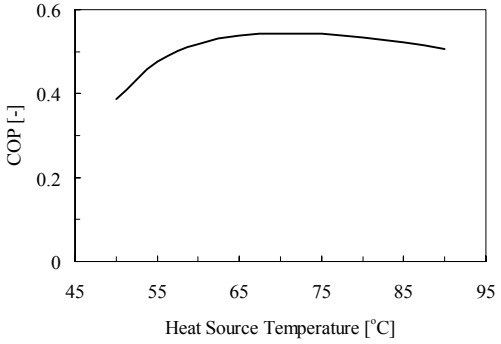

Fig. 3 The effect of heat source temperature on COP.

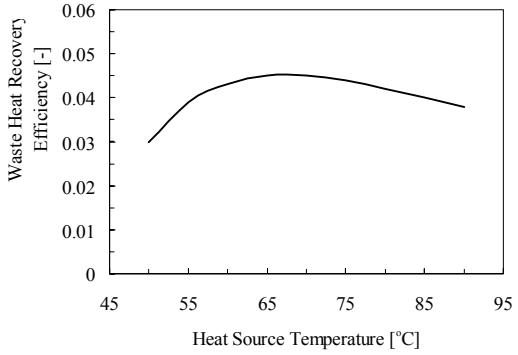

Fig. 4 The effect of heat source temperature on waste heat recovery efficiency.

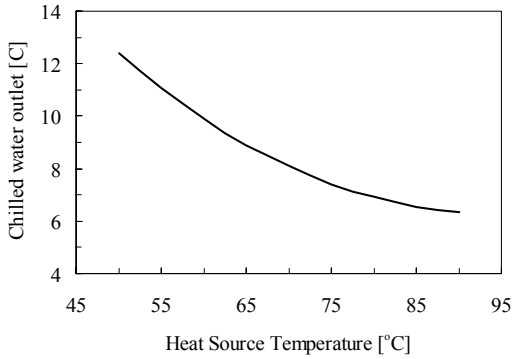

Fig. 5 The effect of heat source temperature on Chilled water outlet temperature.

5.2 Effect of driving heat source temperature on chiller efficiency, η

Figure 4 presents the waste heat recovery efficiency, η, as a function of heat source temperature. For three-bed proposed cycle employing mass recovery scheme with heating/cooling, η rises from 0.03 to 0.046 as hot water inlet temperature is increased from 50 to 65°C with a cooling source 30°C. This is because improvement of cooling capacity of the proposed chiller in this range. It is also observed that η is boosted by about 25% than that of conventional cycle demonstrated in Khan et al. (2005).

5.3 Effect of driving heat source temperature on chilled water outlet temperature

The effect of heat source temperature on average chilled water outlet temperature is depicted in Fig. 5. The chilled water temperature level needs to be considered according to demand side requirement. Mass flow rate of chilled water can control the outlet temperature of chilled water. From Fig. 5, it is seen that the cyclic average chilled water outlet temperature of the proposed cycle decreases with the increase of the driving heat source temperature. Low chilled water outlet temperature is expected from real machine.

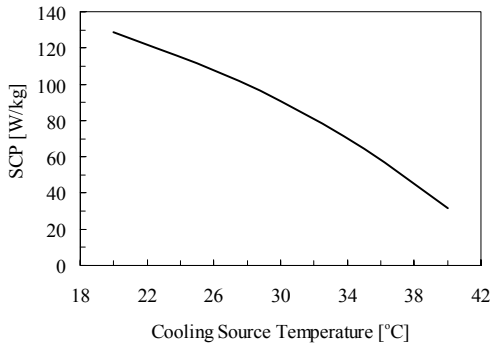

Fig.6 The effect of cooling source temperature on specific cooling power.

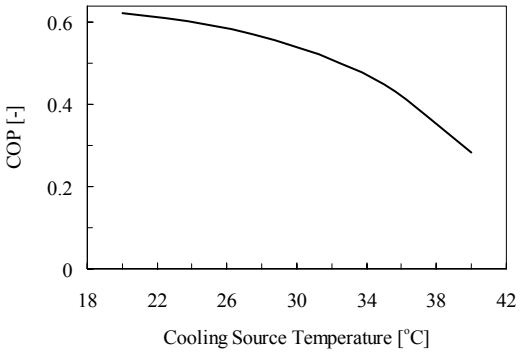

Fig. 7 The effect of cooling source temperature on COP.

5.4 Effect of cooling source temperature on SCP and COP

Figure 6 and 7 show the effect of cooling water inlet temperatures on SCP and COP, respectively. In the present simulation, cooling water mass flow rate into adsorber is taken as 0.4 kg/s, while for the condenser the coolant mass flow rate is taken as 0.34 kg/s. The SCP increases steadily as the cooling water inlet temperature is lowered from 40 to 20°C. This is due to the fact that lower adsorption temperatures result in larger amounts of refrigerant being adsorbed and desorbed during each cycle. The simulated COP values also increase with lower cooling water inlet temperature. For the three bed chiller the COP value reaches 0.62 with 70°C driving source temperature in combination with a coolant inlet temperature of 20°C.

6. Conclusions

A novel three-bed mass recovery chiller with silica gel as adsorbent and water as adsorbate is proposed and the performances are evaluated by numerical technique. For the utilization of the demand, multi-bed mass recovery

cycle is presented and the effects of operating conditions are investigated. The following concluding remarks can be drawn from the present analysis:

(i) The main feature of the proposed chiller is the ability to be driven by relatively low temperature heat source. The chiller can utilize the fluctuated heat source temperature between 50 and 90°C to produce effective cooling along with a coolant inlet at 30°C.

(ii) In the cycle simulation study, hot and cooing water temperatures are the most influential parameters. SCP increases with the increase of hot water temperature and opposite tendency for cooling water temperature. Highest COP value is obtained for hot water temperature variation from 65 to 78°C.

(iii) In the low heat source temperature, COP improves significantly.

(iv) Waste heat recovery efficiency, η rises from 0.03 to 0.046 as hot water inlet temperature is increased from 50 to 65°C with cooling source at 30°C.

(v) Delivered outlet chilled water temperature of the proposed cycle decreases with the increase of driving heat source temperature.

References

Brunauer, S. (1945): The adsorption of gases and vapors, vil.1 Princeton, NJ: Princeton University Press.

Chihara, K. and Suzuki, M. (1983): Air drying by pressure swing adsorption. J. Chem. Eng. Japan, Vol. 16(4), pp. 293-298.

Cacciola, G. and Restuccia, G. (1995): Reversible adsorption heat pump: a thermodynamic model, Int J Refrigeration, Vol. 18, pp. 100–106.

Critoph, R. E. (1998): Forced convection adsorption cycles, Appl Therm Eng, Vol. 18, pp. 799–807.

Douss, N. and Meunier, F. (1989): Experimental study of cascading adsorption cycles, Chem Eng Sci, Vol. 44, pp. 225–235.

Hubard, S. (1954): Equilibrium data for silica gel and water vapor, Ind. Engng Chem., pp. 356-358.

Khan, M. Z. I., Saha, B. B., Alam, K. C. A., Akisawa, A. and Kashiwagi, T. (2005): Performance investigation on mass recovery three-bed adsorption cycle, Proc. of the International Conf. on Mechanical Engineering 2005 (Paper No. ICME2005-TH-03), 28-30 December 2005, Dhaka, BANGLADESH.

Leong, K. C. and Liu, Y. (2004): Numerical study of a combined heat and mass recovery adsorption cooling cycle, Int J Heat Mass Transfer, Vol. 47 (22), pp. 4761–4770.

Miles, D. J. (1989): Analysis and design of a solid adsorption heat driven heat pump, PhD Thesis: Georgia Institute of Technology.

Meunier, F. (1986): Theoretical performances of solid adsorbent cascading cycles using the zeolite-water and active carbonmethanol pairs: four case studies, Heat Recovery CHP Systems, Vol. 6(6), pp. 491–8.

NACC (1992): PTX data for the silica gel/water pair, Manufacturer's proprietary data, Tokyo, Nishiyodo Air Conditioner Co. Ltd.

Pons, M. and Poyelle, F., (1999): Adsorptive machines with advantaged cycles for heat pumping or cooling applications, Int. J. Refrigeration, Vol. 22, pp. 27–37.

Stitou, D, Spinner, B., Satzger, P. and Ziegler, F. (2000): Development and comparison of advanced cascading cycles coupling a solid/gas thermochemical process and a liquid/gas absorption process, Appl Therm Eng, Vol. 20, pp. 1237–1269.

Shelton, S.V., Wepfer, J.W. and Miles, D.J., (1990): Ramp wave analysis of the solid/vapor heat pump, ASME J Energy Resources Technology, Vol. 112, pp. 69–78.

Saha, B. B., Koyama, S., Lee, J. B., Kuwahara, K., Alam, K. C. A., Hamamoto, Y., Akisawa, A. and Kashiwagi, T., (2003): Performance evaluation of a low-temperature waste heat driven multi-bed adsorption chiller, International Journal of Multiphase Flow, Vol. 29, pp. 1249-1263.

Saha, B.B., El-Sharkawy, I.I., Koyama, S., Lee, J.B. and Kuwahara, K. (2006): Waste heat driven multi-bed adsorption chiller: heat exchangers overall thermal conductance on chiller performance, Heat Transfer Engineering, Vol. 28, No. 5, pp. 80-87.

Sakoda, A. and Suzuki, M. (1984): Fundamental study on solar powered adsorption cooling system, J. Chem. Eng. Japan, Vol. 17, pp. 52.

Saha, B. B., Boelman, E. C., Kashiwagi, T. (1995): Computer simulation of a silica gel–water adsorption refrigeration cycle—the influence of operating conditions on cooling output and COP, ASHRAE Trans Res, Vol. 101 (2), pp. 348–357.

Wang, W., Qu, T.F. and Wang, R. Z. (2002): Influence of degree of mass recovery and heat regeneration on adsorption refrigeration cycles, Energy Convers Manage, Vol. 43, pp. 733–741.

Wang, R.Z. (2001): Performance Improvement of Adsorption Cooling by Heat and Mass Recovery Operation, Int. J. Refrigeration, Vol. 24, pp. 602–11.